Electronic Supplementary Material (ESI) for Analyst

Colorimetric quantification of galactose using a nanostructured multi-catalyst system entrapping galactose oxidase and magnetic nanoparticles as peroxidase mimetics

Moon Il Kim[a], *Jongmin Shim*[b], *Taihua Li*[a], *Min-Ah Woo*[a], *Daeyeon Cho*[c], *Jinwoo Lee*[b], *Hyun Gyu Park*[a,*]

Figure S1. X-ray diffraction (XRD) pattern of MMS-40 heat-treated at 400°C (A) and 330°C (B)

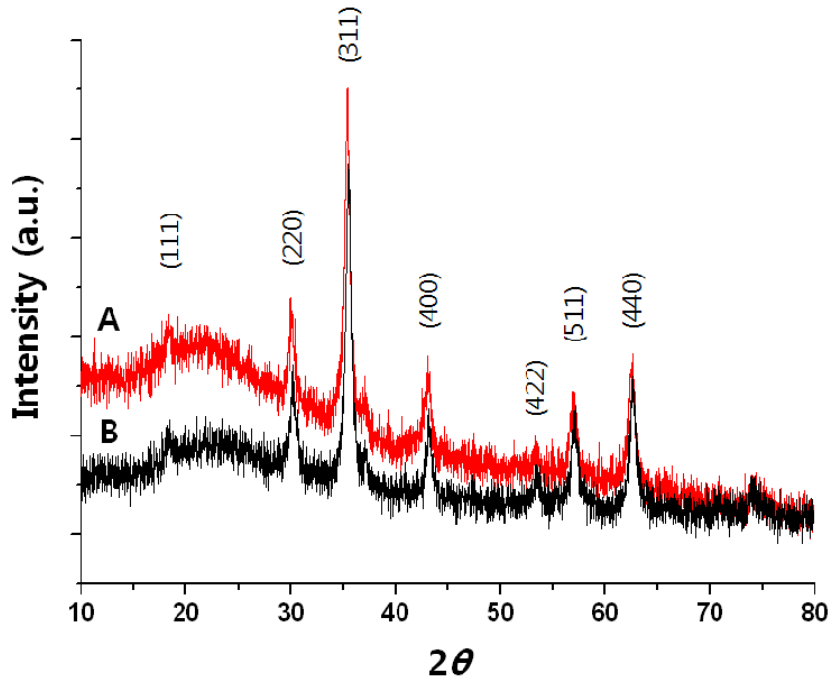

Figure S2. Particle size distributions of MMS-40 obtained using the DLS method.

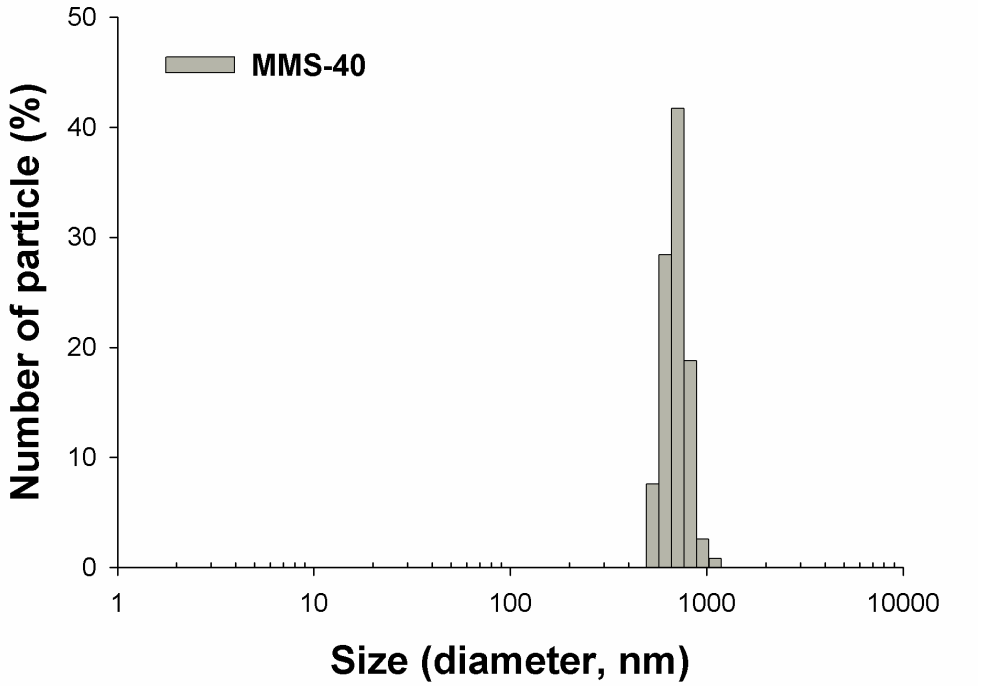

Figure S3. TEM image of MMS-40.

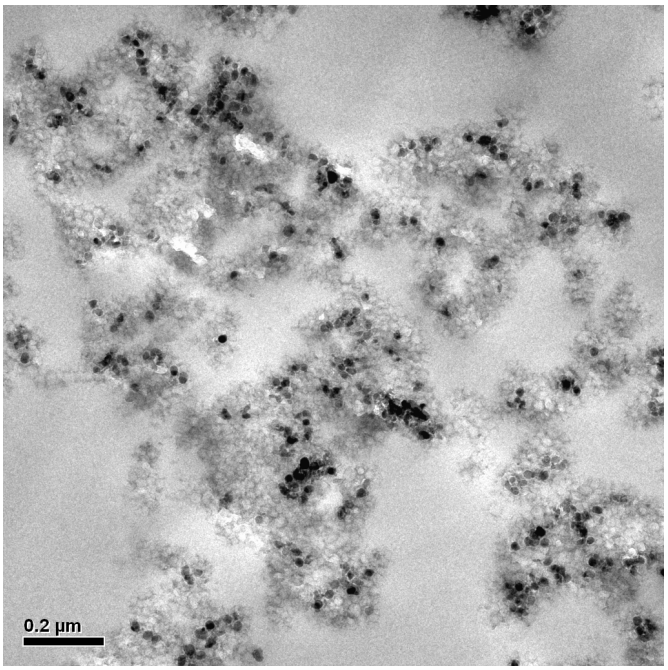

Figure S4. Photograph of the colorimetric detection of galactose using the multi-catalyst systems entrapping Gal Ox in MMS-20 (1), MMS-40 (2), and MMS-60 (3) and the corresponding absorption spectra. ABTS was used as a colorimetric substrate.

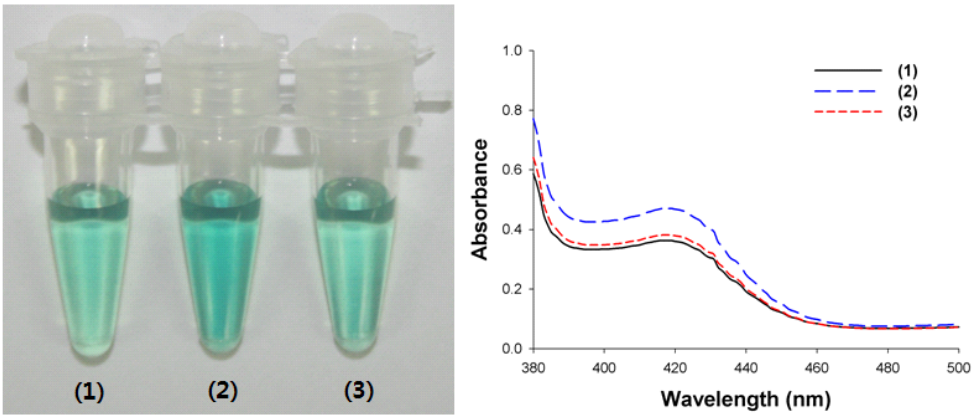

Figure S5. (a) Nitrogen physisorpion isotherms of the multi-catalyst system containing galactose oxidase (MMS/Gal Ox) and bare MMS. **(b)** Pore size distributions of MMS/Gal Ox and bare MMS.

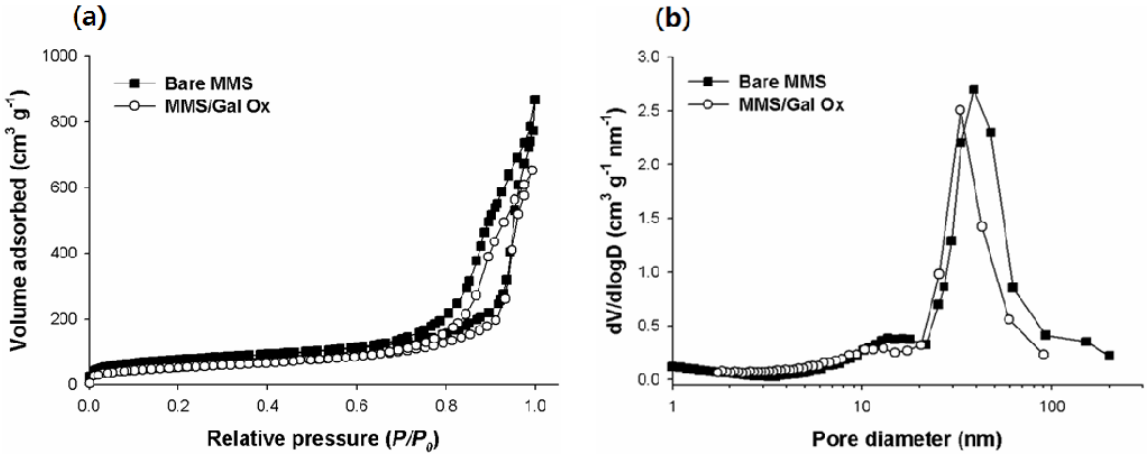

Figure S6. Optimization of **(a)** buffer system (pH, composition, and ionic strength), **(b)** reaction time and the amount of reagents (multi-catalyst and ABTS) by using statistical analysis employing response surface methodology (Box-Behnken model) (Box and Behnken, 1960). Relative activity (%) was determined by using the ratio of the measured activity at each buffer composition to the activity of case 5 (sodium phosphate (10 mM, pH 6.5) + sodium acetate (500 mM, pH 4.0)).

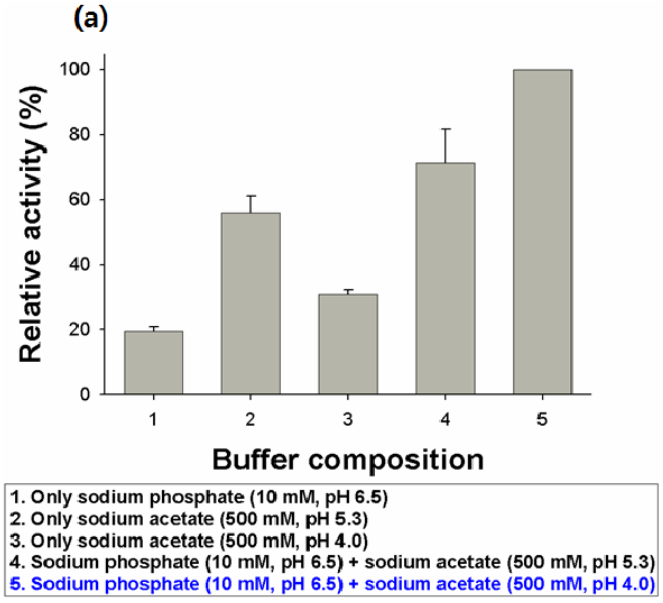

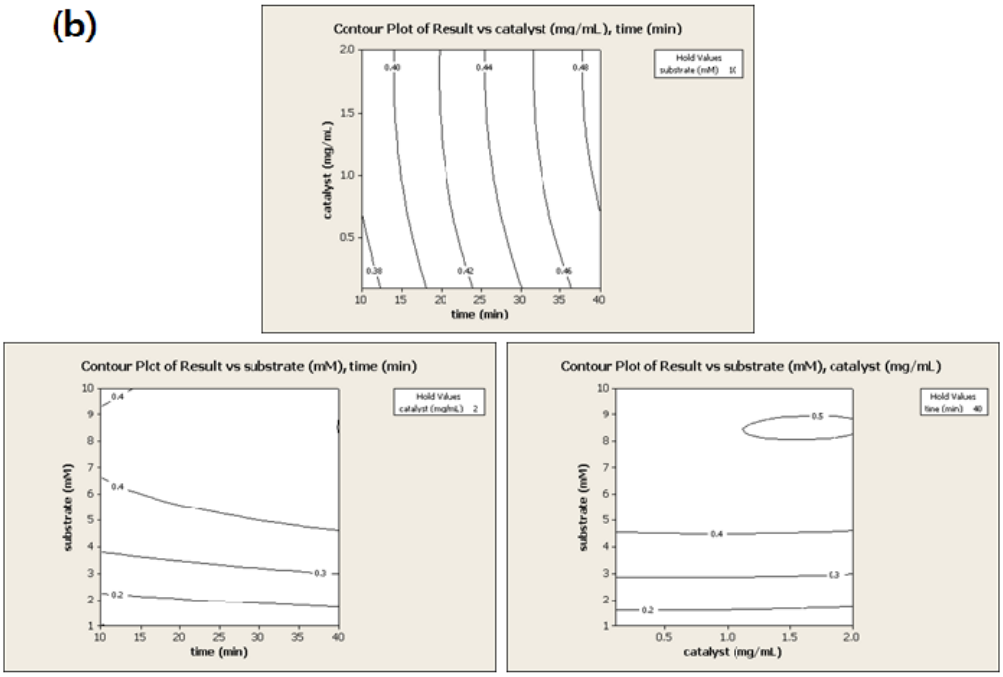

Figure S7. Photograph of the colorimetric detection of galactose using the multi-catalyst system entrapping galactose oxidase in MMS (1), galactose oxidase adsorbed in MMS (2), galactose oxidase covalently attached onto MNPs without silica (3), galactose oxidase physically adsorbed onto MNPs without silica (4), and the corresponding absorption spectra. ABTS was used as a colorimetric substrate.

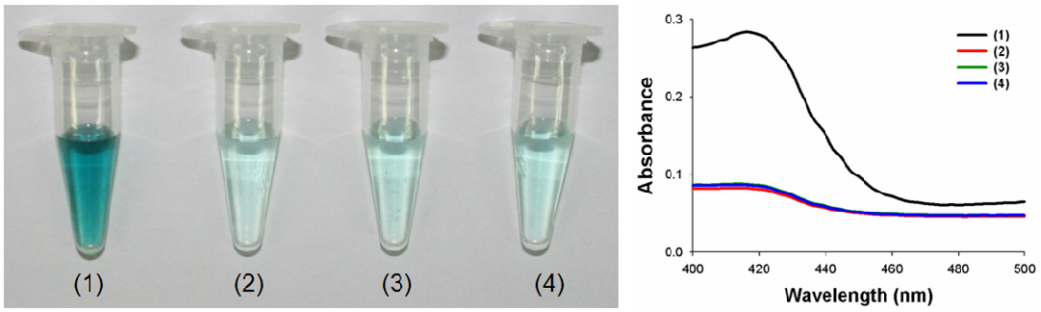

Figure S8. (a) A dose-response curve for galactose detection by using the multi-catalyst system, and **(b)** corresponding linear calibration plot for galactose detection. The error bars represent standard deviations derived from three independent measurements.

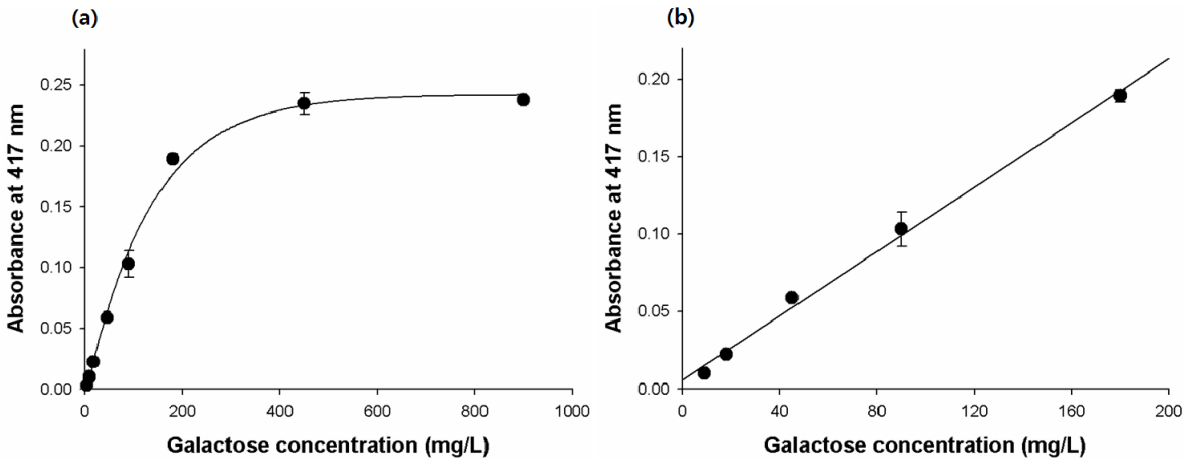

Table S1. Detection precision of the multi-catalyst assay system in a well-plate format for the determination of galactose.

	Sample 1	**Sample 2**	**Sample 3**
Expected galactose (mg/L)	50	100	200
Within-assay			
Average[a] (mg/L)	49.5	102.7	200.6
SD[b]	3.68	6.00	7.50
CV[c] (%)	7.4	5.8	3.7
Recovery[d] (%)	99.04	102.67	100.31
Between-assay			
Average (mg/L)	50.2	102.5	199.6
SD	3.28	4.60	7.71
CV (%)	6.5	4.5	3.9
Recovery (%)	100.50	102.55	99.82

[a] Mean of three independent measurements

[b] Standard deviation of three measurements

[c] Coefficient of variation

[d] Measured value / Expected value x 100

Table S2. Detection precision for Figure 5a.

	Sample 1	**Sample 2**	**Sample 3**	**Sample 4**
Original galactose (mg/L)	24	24	24	24
Added galactose (mg/L)	0	50	150	350
Expected galactose (mg/L)	24	74	174	374
Average[a] (mg/L)	22.4	77.0	169.7	371.5
SD[b]	1.50	4.00	10.3	9.4
CV[c] (%)	6.7	5.2	6.1	2.5
Recovery[d] (%)	93.2	104.0	97.5	99.3

[a] Mean of three independent measurements

[b] Standard deviation of three measurements

[c] Coefficient of variation

[d] Measured value / Expected value x 100

References

G. Box and D. Behnken, *Technometrics*, 1960, **2**, 455–475.